

**SIMULATION ON ATKINSON-MILLER CYCLE
ENGINE OF FOUR STROKE TWO-WHEEL
VEHICLE FOR LIGHT OPERATING
CONDITION**

SOBANA RAJ SUBRAMONIAN

UNIVERSITI SAINS MALAYSIA

2015

**SIMULATION ON ATKINSON-MILLER CYCLE ENGINE OF
FOUR STROKE TWO-WHEEL VEHICLE FOR LIGHT
OPERATING CONDITION**

by

SOBANA RAJ SUBRAMONIAN

**Thesis submitted in fulfillment of the
requirements for the degree of
Master of Science**

October 2015

ACKNOWLEDGEMENT

There are many individuals, who have made the completion of my project is possible, assisted me in various ways. I would like to take this opportunity to express my sincere gratitude to them in here.

I am particularly grateful to my supervisor Dr. Nadiyahnor Md. Yusop, who spared a great amount of valuable time for giving me important guidance, sharing of knowledge and given support throughout my research studies in Universiti Sains Malaysia, Engineering Campus.

I would like to extend my appreciation to Universiti Sains Malaysia, Engineering Campus for giving me this opportunity and providing me a good research environment especially staffs in School of Mechanical Engineering. Special thanks are to Dr.-Ing Muhammad Razi bin Abdul Rahman for providing me guidance over HPC server for ANSYS Fluent use.

Not to forget my friends in School of Mechanical Engineering and other schools for their help and guidance towards completion of this project. My sincere thanks to them, who made my campus life filled with fun and laughter.

Last but not the least and most importantly, my sincere thanks are due to my parents, Mr. A. Subramonian and Mdm. G. Saraswathy, my brother Dr. S. Thrimourthi and Family for their continuous support, borne with me for all these years with love and patience, thanks for giving me freedom to pursue my dreams.

TABLE OF CONTENTS

Acknowledgement.....	ii
Table of Contents	iii
List of Tables.....	vii
List of Figures	viii
List of Abbreviations.....	xvi
List of Symbols	xvii
Abstrak	xviii
Abstract	xx

CHAPTER 1 - INTRODUCTION

1.1 Research Background	1
1.2 Problem Statement.....	8
1.3 Objectives	8
1.4 Scope of Research.....	8

CHAPTER 2 - LITERATURE REVIEW

2.1 Overview.....	9
2.2 Internal Combustion Engine Cycles	10
2.2.1 Otto Cycle	11
2.2.1(a) Time loss	13
2.2.1(b) Heat loss and Exhaust blowdown.....	14
2.2.2 Atkinson Cycle	16
2.2.3 Miller cycle	17
2.3 Compression Ratio.....	22

2.4	Malaysian Drive Cycle Distribution.....	25
2.5	Light and Heavy Load Operating Condition	26
2.6	Summary.....	28

CHAPTER 3 - METHODOLOGY

3.1	Overview.....	29
3.2	Research Flow	30
3.3	Modenas CT110 Engine data	31
3.3.1	Engine Performance Data	32
3.4	Thermodynamics gas cycle analysis.....	32
3.4.1	Thermodynamic Analysis of Air – Standard Otto Cycle.....	32
3.4.2	Thermodynamic Analysis of Air – Standard Over Expanded Engine Cycle	33
3.5	Engine Gas Cycle Simulation Using Ricardo WAVE.....	35
3.5.1	Model Set Up	35
3.5.2	Model Calibration	39
3.5.2(a)	Brake Power & Torque Calibration	39
3.5.3	Investigation Parameters.....	40
3.5.3(a)	Over Expanded Engine Cycle Application	40
3.5.3(b)	High Compression Ratio Application	41
3.6	Engine Combustion Simulation by CFD Method.....	42
3.6.1	Model Verification.....	42
3.6.1(a)	Mesh Model.....	42
3.6.1(b)	Computational Fluid Dynamic Method.....	44
3.6.1(c)	Numerical Method.....	48
3.6.2	Model Setup	52

3.6.2(a) Spark Ignition	52
3.6.2(b) Material Selection	53
3.6.2(c) Boundary Condition	55
3.6.2(d) In –Cylinder and Dynamic Mesh Zones setup	56
3.6.3 Model Validation	58
3.6.4 Investigation Parameters	58
3.6.4(a) Over Expanded Engine Cycle Application	58
3.6.4(b) High Compression Ratio Application	58

CHAPTER 4 - RESULT AND DISCUSSION

4.1 Overview.....	59
4.2 The Advantages and Disadvantages of Over Expanded Engine Cycle Method Based on Thermodynamic Gas Cycle Analysis.....	59
4.3 Verification and Validation	64
4.3.1 Model Calibration of Engine Gas Cycle Simulation	64
4.3.2 Model Verification and Validation of Engine Combustion Simulation by CFD Method	66
4.3.2(a) Model Verification using Engine In – Cylinder Data	73
4.3.3 In-Cylinder Data Validation at Various Engine Cycle Ratio	75
4.4 Premature Combustion Investigation by CFD Method	77
4.5 Over Expanded Engine Cycle at 9.3:1 of Compression Ratio.....	86
4.5.1 Effect of LIVC and LEVO on Engine Heat Transfer Coefficient	87
4.5.2 Effect of LIVC and LEVO on Engine Brake Power, Torque, BSFC and Brake Thermal Efficiency	90
4.6 Over Expanded Engine cycle at Various Compression Ratio	93

4.6.1	Effect of High Compression ratio on In-cylinder gas Density, Pressure and Engine Heat Transfer	94
4.6.2	Effect of High Compression Ratio on A10M15 Engine Brake Power, Torque, BSFC and Brake Thermal Efficiency.....	97
4.6.3	Effect of High Compression Ratio on A10M30 Engine Performance and Engine In-cylinder Gas Density and Engine Heat Transfer Rate.....	101
4.7	Engine Performance Over Vehicle Speed and Load	105
4.7.1	Light and Heavy Load Condition at Suburban, and Urban Cruising Speed.....	105
4.7.2	Light and Heavy Load Condition at Highway Cruising Speed	111
4.7.3	Engine Optimization For Best Engine Efficiency	113
4.8	Effect of Optimized Engine on The Engine Heat Transfer Coefficient	115
4.9	Effect of Optimized Engine on Emissions	117
 CHAPTER 5 - CONCLUSIONS		
5.1	Conclusions	119
5.2	Future Recommendation Work	121
REFERENCES.....		123
 APPENDICES		

LIST OF TABLES

		Page
Table 2.1	Conversion of characterized compression ratio to cycle ratio	20
Table 2.2	Approximate value of motorcycle speed of various drive cycle pattern (Jih Houh 2012)	26
Table 2.3	Parameters used for cruising power output prediction (Jih Houh 2012) for light load (best case) and heavy load (worst case)	27
Table 3.1	Modenas CT110 engine parameters	31
Table 3.2	Maximum brakepower and maximum torque (extracted from CT110 Prospectus)	32
Table 3.3	Engine parameters for air-standard cycle theoretical calculation	33
Table 3.4	Fuel properties (Benajes et al. 2014; Masum et al. 2015)	36
Table 3.5	Dynamic Mesh method selection and value input in ANSYS Fluent	46
Table 3.6	Mass fraction values for fresh gas mixture	53
Table 3.7	Burned/residual gas fraction, X_r	53
Table 3.8	Mass fraction values for fresh and residual gas mixture	54
Table 4.1	Average surface temperature of engine in – cylinder surfaces for Ricardo WAVE input	66
Table 4.2	Mesh sizing selected for mesh independent study	71
Table 4.3	ANSYS Fluent monitor points at 100 iteration of simulation using various mesh sizes	72
Table 4.4	Maximum allowable compression ratio (RC) for engine model Atkinson cycle 10 degree LEVO (A10), Miller cycle 15 & 30 degree LIVC (M15 & M30)	86

LIST OF FIGURES

		Page
Figure 1.1	Total Vehicle and Motorization index in ASEAN, China and India (Silitonga et al. 2012)	1
Figure 1.2	Motorcycles and car ownership in Malaysia (Asean Japan Transportation Partnership 2014)	2
Figure 1.3	Final consumption of Petroleum Products and Crude Oil production in Malaysia (MEIH 2011)	2
Figure 1.4	Total World and Asia Pacific Crude oil production and consumption between 1980 and 2013 (BP Global 2015)	3
Figure 1.5	Mazda's 2.3 liters Miller Cycle engine (Grueninger 2007)	6
Figure 2.1	p-V diagram of air-standard Otto cycle (Ganeson 2007)	11
Figure 2.2	Losses illustration on p-V diagram (Taylor 1985)	14
Figure 2.3	Illustration of Atkinson cycle concept on p-V diagram	16
Figure 2.4	Work output comparison between Otto and Atkinson cycle (Hou 2007)	17
Figure 2.5	Variation of the displacement volume to obtain maximum efficiency according to vehicle speed at same load (Kutlar et al. 2005)	18
Figure 2.6	Brake Specific Fuel Consumption Vs Engine Speed at various engine loads (Iskandar & Heoy 2014)	19
Figure 2.7	p-V diagram of air-standard Miller cycle	20
Figure 2.8	Influence of characterized compression ratio, γ and compression ratio, γ_c on temperature at point 4 and 5 (Lin et al. 2014)	20
Figure 2.9	Temperature versus Compression ratio Ge et al. (2005b)	24
Figure 2.10	Malaysian drive cycle pattern for urban, suburban, rural and highway cruising (Jih Houh 2012)	25
Figure 2.11	Cruising power versus speed for light and heavy load condition (Jih Houh 2012)	27
Figure 3.1	Research methodology flow chart	30
Figure 3.2	Air – standard over expanded engine cycle	34

Figure 3.3	Engine map of Modenas CT110 engine configuration in Ricardo WAVE	35
Figure 3.4	Fuel injector linked to throttle body which represents carburetor function in Ricardo WAVE	36
Figure 3.5	Fuel injector value input panel in Ricardo WAVE	37
Figure 3.6	Burned air and burned fuel fraction set up in Ricardo WAVE	37
Figure 3.7	Engine geometry configuration in Ricardo WAVE	38
Figure 3.8	Heat transfer configuration in Ricardo WAVE	38
Figure 3.9	Combustion model configuration in Ricardo WAVE	39
Figure 3.10	Multiple case simulation value input in Ricardo WAVE	40
Figure 3.11	Intake and exhaust valve profile of over expanded engine cycles and Otto cycle	41
Figure 3.12	Structured Hexahedral mesh	43
Figure 3.13	Structured Hexahedral mesh for layering zone	43
Figure 3.14	Species model setup in ANSYS Fluent	45
Figure 3.15	Solution method selection in ANSYS Fluent	47
Figure 3.16	Spark ignition setup in ANSYS FLUENT	52
Figure 3.17	Reaction configuration in ANSYS Fluent	55
Figure 3.18	Boundary Zone Selection in ANSYS Mesh Application, ICEM CFD	56
Figure 3.19	In-Cylinder dynamic mesh setup in ANSYS Fluent	56
Figure 3.20	Dynamic Mesh Zones tab for the piston motion setup in ANSYS Fluent	57
Figure 4.1	Exhaust gas temperature of various engine cycles against compression ratio	60
Figure 4.2	Thermal efficiency of various engine cycle against compression ratio	61
Figure 4.3	Brake Power of various engine cycle against compression ratio	61

Figure 4.4	Brake Specific Fuel Consumption of various engine cycle against compression ratio	62
Figure 4.5	Ricardo WAVE Engine setup calibration using engine brake power data	64
Figure 4.6	Ricardo WAVE Engine setup calibration using engine brake engine torque data	65
Figure 4.7	J configuration for Air Fuel Ratio and Combustion Duration input in Ricardo WAVE software setup	65
Figure 4.8	Surface temperature of engine in-cylinder surfaces against number of simulations	66
Figure 4.9	ANSYS Fluent residual graph of simulation using various mesh sizes based on SIMPLE algorithm – a) CoarseSIMPLE, b) MediumSIMPLE and c) FineSIMPLE	68
Figure 4.10	Five different mesh sizing of CT110 engine combustion chamber model – a) coarse mesh, b) coarse – medium mesh, c) Medium mesh, d) Medium – Fine mesh and e) Fine mesh	69
Figure 4.11	Distorted mesh cell of combustion chamber model at different location	69
Figure 4.12	ANSYS Fluent residual graph based on fine and highly skewed mesh model simulation using two different algorithm – a) FineSIMPLE and b) FinePISO	70
Figure 4.13	Engine in-cylinder pressure graph of various mesh models compared to Ricardo WAVE pressure data	73
Figure 4.14	Engine In-cylinder peak pressure difference between WAVE and Fluent result of various mesh sizes	74
Figure 4.15	In-cylinder density comparison between WAVE and Fluent model at compression ratio of 9.3 (RC9.3) of engine model Atkinson cycle 10 degree LEVO (A10), Miller cycle 15 & 30 degree LIVC (M15 & M30)	75
Figure 4.16	In-cylinder gas pressure comparison at compression ratio of 9.3 (RC9.3) of engine model Atkinson cycle 10 degree LEVO (A10), Miller cycle 15 & 30 degree LIVC (M15 & M30)	76
Figure 4.17	In-cylinder gas temperature comparison at compression ratio of 9.3 (RC9.3) of engine model Atkinson cycle 10 degree LEVO (A10), Miller cycle 15 & 30 degree LIVC (M15 & M30)	76

Figure 4.18	Engine combustion chamber interior gas temperature contour with fuel knock visible at various locations	78
Figure 4.19	Interior gas temperature contour of Standard Modenas CT110 engine combustion chamber at a) 294.50 degree of crank angle, b) 325.75 degree of crank angle, c) 347.25 degree of crank angle and d) 354.00 degree of crank angle	79
Figure 4.20	Interior gas temperature contour of Modenas CT110 engine combustion chamber with compression ratio of 10:1 at a) 352.75 degree of crank angle, b) 353.25 degree of crank angle, c) 360.00 degree of crank angle and d) 364.00 degree of crank angle	80
Figure 4.21	Interior gas temperature contour of Modenas CT110 engine combustion chamber with compression ratio of 11:1 at a) 345.50 degree of crank angle, b) 354.50 degree of crank angle and with compression ratio of 12:1 at c) 342.75 degree of crank angle and d) 353.75 degree of crank angle	81
Figure 4.22	Ricardo WAVE simulation result of engine heat transfer rate graph of various compression ratio (RC9.3 – RC13) of engine model Atkinson cycle 10 degree LEVO (A10), Miller cycle 15 & 30 degree LIVC (M15 & M30) from 30 to 180 degrees of crank angle	83
Figure 4.23	Interior gas temperature contour of Atkinson cycle 10 degree LEVO and Miller cycle 15 degree LIVC (A10M15) engine combustion chamber with compression ratio of 11:1 at a) 345.50 degree of crank angle, b) 354.50 degree of crank angle, c) 342.75 degree of crank angle, d) A10M15 engine with compression ratio of 12:1	84
Figure 4.24	Interior gas temperature contour of Atkinson cycle 10 degree LEVO and Miller cycle 30 degree LIVC (A10M30) engine combustion chamber with compression ratio of 12:1 at a) 337.75degree of crank angle, b) 350.00 degree of crank angle and c) 354.00 degree of crank angle	85
Figure 4.25	In-cylinder total mass at 9.3:1 of compression ratio of engine model Otto cycle, Atkinson cycle 10 degree LEVO (A10), Miller cycle 15 & 30 degree LIVC (M15 & M30)	87
Figure 4.26	In-cylinder Combustion Heat Release Rate at compression ratio of 9.3:1 of engine model Otto cycle, Atkinson cycle 10 degree LEVO (A10), Miller cycle 15 & 30 degree LIVC (M15 & M30)	88

Figure 4.27	Engine Heat Transfer Rate of engines at compression ratio of 9.3:1 of engine model Otto cycle, Atkinson cycle 10 degree LEVO (A10), Miller cycle 15 & 30 degree LIVC (M15 & M30)	88
Figure 4.28	Engine Heat Transfer Coefficient at compression ratio of 9.3:1 of engine model Otto cycle, Atkinson cycle 10 degree LEVO (A10), Miller cycle 15 & 30 degree LIVC (M15 & M30)	89
Figure 4.29	Brake Power curve of engines at compression ratio of 9.3:1 of engine model Otto cycle, Atkinson cycle 10 degree LEVO (A10), Miller cycle 15 & 30 degree LIVC (M15 & M30)	91
Figure 4.30	Brake Engine Torque curve engines at compression ratio of 9.3:1 of engine model Otto cycle, Atkinson cycle 10 degree LEVO (A10), Miller cycle 15 & 30 degree LIVC (M15 & M30)	91
Figure 4.31	Brake Specific Fuel Consumption curve engines at compression ratio of 9.3:1 of engine model Otto cycle, Atkinson cycle 10 degree LEVO (A10), Miller cycle 15 & 30 degree LIVC (M15 & M30)	92
Figure 4.32	Brake Thermal Efficiency curve of engines at compression ratio of 9.3:1 of engine model Otto cycle, Atkinson cycle 10 degree LEVO (A10), Miller cycle 15 & 30 degree LIVC (M15 & M30)	93
Figure 4.33	In-cylinder Gas Density of engine model Otto cycle, Atkinson cycle 10 degree LEVO (A10), Miller cycle 15 degree LIVC (M15) at various compression ratios (RC9.3 – RC13)	94
Figure 4.34	In-cylinder Gas Pressure of engine model Otto cycle, Atkinson cycle 10 degree LEVO (A10), Miller cycle 15 degree LIVC (M15) at various compression ratios (RC9.3 – RC13)	95
Figure 4.35	Engine Heat Transfer Rate of engine model Otto cycle, Atkinson cycle 10 degree LEVO (A10), Miller cycle 15 degree LIVC (M15) at various compression ratios (RC9.3 – RC13)	95
Figure 4.36	Engine Heat Transfer Coefficient of engine model Otto cycle, Atkinson cycle 10 degree LEVO (A10), Miller cycle 15 degree LIVC (M15) at various compression ratios (RC9.3 – RC13)	96

Figure 4.37	In-cylinder Gas Temperature of engine model Otto cycle, Atkinson cycle 10 degree LEVO (A10), Miller cycle 15 degree LIVC (M15) at various compression ratios (RC9.3 – RC13)	97
Figure 4.38	Brake Power graph of engine model Otto cycle, Atkinson cycle 10 degree LEVO (A10), Miller cycle 15 degree LIVC (M15) at various compression ratios (RC9.3 – RC13)	98
Figure 4.39	Brake Thermal Efficiency graph of engine model Otto cycle, Atkinson cycle 10 degree LEVO (A10), Miller cycle 15 degree LIVC (M15) at various compression ratios (RC9.3 – RC13)	99
Figure 4.40	Brake Specific Fuel Consumption graph of engine model Otto cycle, Atkinson cycle 10 degree LEVO (A10), Miller cycle 15 degree LIVC (M15) at various compression ratios (RC9.3 – RC13)	99
Figure 4.41	Brake Engine Torque graph of engine model Otto cycle, Atkinson cycle 10 degree LEVO (A10), Miller cycle 15 degree LIVC (M15) at various compression ratios (RC9.3 – RC13)	100
Figure 4.42	Brake Thermal Efficiency graph of engine model Otto cycle, Atkinson cycle 10 degree LEVO (A10), Miller cycle 30 degree LIVC (M30) at various compression ratios (RC9.3 – RC13)	102
Figure 4.43	In-cylinder Gas Temperature of engine model Otto cycle, Atkinson cycle 10 degree LEVO (A10), Miller cycle 30 degree LIVC (M30) at various compression ratios (RC9.3 – RC13)	103
Figure 4.44	In-cylinder Gas Density of engine model Otto cycle, Atkinson cycle 10 degree LEVO (A10), Miller cycle 30 degree LIVC (M30) at various compression ratios (RC9.3 – RC13)	103
Figure 4.45	Brake Engine Torque graph of engine model Otto cycle, Atkinson cycle 10 degree LEVO (A10), Miller cycle 30 degree LIVC (M30) at various compression ratios (RC9.3 – RC13)	104
Figure 4.46	Brake Power required at suburban and urban cruising speed of engine model Otto cycle, Atkinson cycle 10 degree LEVO (A10), Miller cycle 15 & 30 degree LIVC (M15 & M30)	106

Figure 4.47	Fuel consumption rate graph of engine model Otto cycle, Atkinson cycle 10 degree LEVO (A10), Miller cycle 15 & 30 degree LIVC (M15 & M30) at compression ratio of 11:1	107
Figure 4.48	Fuel consumption rate by engine cycle – Otto cycle, Atkinson cycle 10 degree LEVO, Miller cycle 15 & 30 degree LIVC (M15 & M30) at light load condition and suburban and urban cruising speed	107
Figure 4.49	Fuel consumption rate by engine cycle – Otto cycle, Atkinson cycle 10 degree LEVO, Miller cycle 15 & 30 degree LIVC (M15 & M30) at heavy load condition and suburban and urban cruising speed	108
Figure 4.50	Brake Specific Fuel Consumption graph of engine model Otto cycle, Atkinson cycle 10 degree LEVO (A10), Miller cycle 15 & 30 degree LIVC (M15 & M30) at compression ratio of 11:1	109
Figure 4.51	Brake Thermal Efficiency graph of engine model Otto cycle, Atkinson cycle 10 degree LEVO (A10), Miller cycle 15 & 30 degree LIVC (M15 & M30) at compression ratio of 11:1	109
Figure 4.52	BSFC improvement of Atkinson cycle 10 degree LEVO (A10) with Miller cycle 15 degree LIVC (M15) engine over Otto cycle engine	110
Figure 4.53	Brake Engine Torque graph of engine model Otto cycle, Atkinson cycle 10 degree LEVO (A10), Miller cycle 15 & 30 degree LIVC (M15 & M30) at compression ratio of 11:1	111
Figure 4.54	Brake Power required at highway cruising speed for the engine model Otto cycle, Atkinson cycle 10 degree LEVO (A10), Miller cycle 15 & 30 degree LIVC (M15 & M30) at a compression ratio of 11:1	112
Figure 4.55	Fuel consumption rate by engine cycle – Otto cycle, Atkinson cycle 10 degree LEVO, Miller cycle 15 & 30 degree LIVC (M15 & M30) at light load condition and highway cruising speed	113
Figure 4.56	Fuel consumption rate by engine cycle – Otto cycle, Atkinson cycle 10 degree LEVO, Miller cycle 15 & 30 degree LIVC (M15 & M30) at heavy load condition and highway cruising speed	113
Figure 4.57	Engine Heat Transfer Coefficient of Otto cycle and Atkinson cycle 10 degree LEVO (A10) with Miller cycle 15 degree LIVC (M15) engine at compression ratio of 11:1	115

Figure 4.58	In-cylinder Combustion Heat Release Rate of Otto cycle and Atkinson cycle 10 degree LEVO (A10) with Miller cycle 15 degree LIVC (M15) engine at compression ratio of 11:1	116
Figure 4.59	Carbon Monoxide concentration of Otto cycle and Atkinson cycle 10 degree LEVO (A10) with Miller cycle 15 degree LIVC (M15) engine at compression ratio of 11:1	117
Figure 4.60	<i>NO_x</i> concentration of Otto cycle and Atkinson cycle 10 degree LEVO (A10) with Miller cycle 15 degree LIVC (M15) engine at compression ratio of 11:1	118

LIST OF ABBREVIATIONS

AFR or A/F Ratio	Air Fuel Ratio
BDC	Bottom Dead Center
BSFC	Brake Specific Fuel Consumption
cc	Cubic Centimeter
CO ₂	Carbon Dioxide
EEVO	Early Exhaust Valve Opening
EIVC	Early Intake Valve Closing
H ₂ O	Hydrogen Dioxide
LEVO	Late Exhaust Valve Opening
LIVC	Late Intake Valve Closing
NO _x	Nitrogen Oxides
O ₂	Oxygen
OEE	Over Expanded Engine
PISO	Pressure-Implicit with Splitting of Operators
PPM	Parts Per Million
RON	Research Octane Number
RPM	Revolution Per Minute
SIMPLE	Semi-Implicit Method for Pressure-Linked Equations
SIMPLEC	SIMPLE Consistent
TDC	Top Dead Center
UDF	User Define Function

LIST OF SYMBOLS

Symbol	Definition	Unit
C_v	Specific heat value	kJ/kg K
G_f	Fresh gas percentage	
k	Specific heat ratio	
M_t	Total mass	
M_f	Fuel mass	
M_a	Air mass	
M_{ex}	Exhaust Gas Mass	
N	Revolution per second	rev/s
n	Number of revolution per cycle	
P	Pressure in the cylinder	kPa
R	Gas constant	kJ/kg K
R_e	Expansion ratio	
R_c	Compression ratio	
T	Temperature in the cylinder	K
V_d	Displacement volume	m ³
V_c	Clearance volume	m ³
V_{exp}	Expanded volume	m ³
W	Work	kJ/kg
X_r	Residual gas percentage	
<i>Subscript</i> <i>1,2,3,4</i>	Label on p-V diagram	
<i>do, co</i>	Volumes of Otto cycle	
<i>dm, cm</i>	Volumes of Miller cycle	

SIMULASI KITAR ENJIN ATKINSON-MILLER DALAM ENJIN EMPAT LEJANG KENDERAAN DUA RODA UNTUK PENGOPERASIAN RINGAN

ABSTRAK

Enjin asal motosikal adalah berdasarkan pada kitar Otto. Enjin kitar Otto hanya menggunakan kuasa yang dihasilkan dengan efisien pada keadaan pengoperasian kenderaan yang berat seperti berat keseluruhan maksimum, tekanan tayar yang rendah dan luas kawasan rintangan yang maksimum. Hasilnya, kuasa maksimum ini telah dibazirkan untuk pengoperasian ringan. Disebabkan oleh strok lejang kuasa yang agak terhad dalam kitar Otto, haba yang diperoleh tidak dapat digunakan sepenuhnya. Justeru, haba yang masih terdapat di kebuk pembakaran disingkirkan melalui ekzos dan sistem penyejukan enjin. Tetapi, aplikasi kitar enjin Atkinson-Miller dengan nisbah mampatan yang tinggi dapat menyelesaikan masalah ini. Objektif analisis ini adalah untuk menyiasat hasil yang diperoleh daripada aplikasi kitar enjin Atkinson-Miller dengan nisbah mampatan yang tinggi pada enjin motosikal. Penyelidikan ini melibatkan analisis satu dimensi yang menggunakan perisian Ricardo WAVE untuk memperoleh data supaya kelebihan dan keburukan aplikasi nisbah mampatan yang tinggi pada enjin petrol kitar Atkinson-Miller boleh diramalkan. Selanjutnya, analisis tiga dimensi dilakukan dengan menggunakan perisian ANSYS Fluent untuk menjalankan siasatan terutamanya ketukan enjin yang berlaku disebabkan oleh tekanan mampatan yang tinggi. Selain itu, simulasi tiga dimensi dapat meramalkan ketumpatan gas, tekanan gas dan suhu gas. Didapati bahawa, kehilangan haba melalui blok enjin dan ditambah pula dengan gas ekzos yang bersuhu tinggi disingkirkan melalui ekzos mengurangkan keseluruhan kerja bersih dan kecekapan haba. Jumlah haba yang disingkirkan melalui ekzos oleh enjin kitar Atkinson-Miller adalah kurang berbanding enjin kitar Otto disebabkan oleh strok

lejang kuasa yang lebih lama. Walaubagaimanapun, penggunaan konsep enjin kitar Miller dalam enjin kitar Atkinson-Miller, menyebabkan enjin mengalami kemerosotan dalam kuasa brek, kuasa tork dan kecekapan terma brek. Oleh itu, kuasa brek dan tork yang rendah adalah kelemahan yang dikesan pada enjin kitar Atkinson-Miller tetapi, kuasa brek dan tork meningkat secara drastik selepas nisbah mampatan enjin ditingkatkan kepada 20:1. Namun sedemikian, analisis tiga dimensi mendapati enjin kitar Atkinson-Miller mengalami masalah ketukan enjin bagi nisbah mampatan melebihi 11:1. Aplikasi enjin kitar Atkinson-Miller sahaja tidak mencukupi. Tetapi, dengan nisbah mampatan sehingga 11:1, enjin kitar Atkinson-Miller mempunyai keupayaan pada penggunaan bahan-api dengan efisien untuk pengoperasian ringan seperti berat keseluruhan yang minimum, tekanan tayar yang optimum dan luas kawasan rintangan yang minimum. Didapati bahawa, aplikasi enjin kitaran Atkinson-Miller (10 darjah LEVO dan 15 darjah LIRC) pada nisbah mampatan 11:1 (A10M15_RC11) mengurangkan penggunaan bahan api sebanyak 1 peratus pada pengoperasian ringan dan 5 peratus pada pengoperasian yang berat pada corak pemanduan di pinggir Bandar dan luar Bandar. Untuk corak pemanduan di lebuh raya, penggunaan bahan api dikurangkan sebanyak 2.9 peratus hingga 3 peratus pada keadaan pengoperasian yang ringan dan berat. Walau bagaimanapun, kitaran enjin A10M15_RC11 mengalami kadar pemindahan haba yang tinggi semasa lejang mampatan dan pembakaran dalam enjin jika dibandingkan dengan enjin kitar Otto tetapi mempunyai kadar pemindahan haba yang rendah semasa lejang kuasa dan ekzos yang mengurangkan suhu gas semasa lejang masukan. Kesimpulannya, kitar enjin A10M15_RC11 mempunyai kecekapan terma brek yang tinggi dan penggunaan bahan api yang rendah pada keadaan pengoperasian ringan dan berat.

SIMULATION ON ATKINSON-MILLER CYCLE ENGINE OF FOUR STROKE TWO-WHEEL VEHICLE FOR LIGHT OPERATING CONDITION

ABSTRACT

Standard engine found in motorcycles are based on Otto cycle. The Otto cycle engine utilize the maximum amount of power is found to be efficient only at heavy operating condition such as maximum total mass, low tire pressure and maximum drag due to maximum frontal area. Consequently, this maximum power has been wasted for the light operating condition usage. Due to short expansion stroke in the Otto cycle, the system was unable to fully utilize the heat generated. Hence, extra heat has been ejected to the environment through the exhaust and engine block cooling system. However, the Atkinson-Miller cycle engine application with higher compression ratio is able to solve the problem. The objective is to investigate the behavior of the Atkinson-Miller cycle spark ignition engine with high compression ratio of a motorcycle engine. This research involves one dimensional analysis using Ricardo WAVE to find the engine output data and the advantage and disadvantages of having high compression ratio of the Atkinson-Miller cycle spark ignition engine can be predicted. Further to this, three dimensional analysis is performed using ANSYS Fluent to conduct the investigation mainly on fuel knocking due to high compression pressure. The three dimensional simulations predict on the gas density, gas pressure and gas temperature profile. It has been found that, an increase in the heat flux through engine block coupled with high temperature exhaust gas exiting the exhaust port consequently decreases both total net work output and the thermal efficiency. The amount of heat ejected through the exhaust is lower in the Atkinson-Miller cycle engine compared to the Otto cycle engine mainly due to the greater expansion. However, with the application of the Miller cycle concept in the over expanded cycle,

the engine experiences losses in brake power, brake engine torque and brake thermal efficiency. The low torque and lower brake power is found to be downside of this Atkinson-Miller cycle engine but, the brake power and torque drastically improved after engine compression ratio increased to 20:1. However, three dimensional analysis of the Atkinson-Miller cycle found the engine to experience fuel knocking for compression ratio above 11:1. Consequently, the stand alone operation of Atkinson-Miller cycle is insufficient. Therefore, the Atkinson-Miller cycle engine are coupled with high compression ratio, 11:1. The high compression ratio Atkinson-Miller cycle engine has improved fuel consumption for light load/operating condition (minimum total mass, optimum tire pressure and minimum drag due to minimum frontal area). The Atkinson-Miller cycle engine (10 degree LEVO and 15 degree LIVC) at compression ratio of 11:1 (A10M15_RC11) reduces fuel consumption by 1 percent at light load and 5 percent at heavy load condition for suburban and urban drive pattern. For highway drive pattern, fuel consumption reduced by 2.9 to 3 percent for both load condition. However, A10M15_RC11 cycle engine experiences high heat transfer rate during compression stroke and combustion compared to the Otto cycle engine but has low heat transfer rate during power and exhaust stroke which reduces intake gas temperature. This situation concludes that, A10M15_RC11 cycle engine has low fuel consumption and high brake thermal efficiency for both load conditions.

CHAPTER 1

INTRODUCTION

1.1 Research Background

Petrol price goes up every year due to increasing demand for petrol. For developing countries, personal vehicles such as motorcycles and cars are preferred due to a lack of proper public transportation (Pongthanaisawan & Sorapipatana 2010). Hence, as shown in Figure 1.1, total number of vehicles increases approximately by 43 percent from year 2005 to 2008 and expected to increase approximately by 46 percent from year 2008 to 2015 in ASEAN countries.

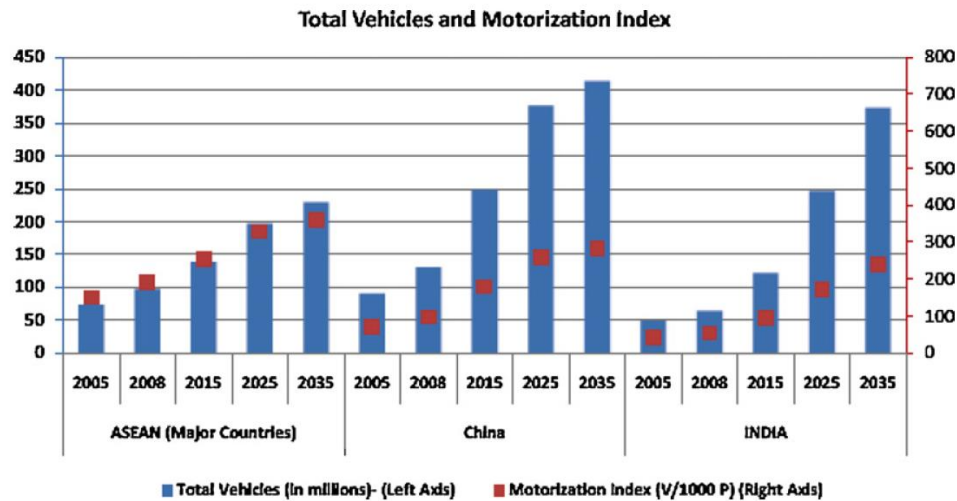


Figure 1.1: Total Vehicle and Motorization index in ASEAN, China and India (Silitonga et al. 2012)

Among the personal vehicles, motorcycles are most favored in developing countries due to vehicle ownership cost and high petrol price. Besides owning cost and petrol price, maintenance cost is another reason as motorcycles exhibit lowest maintenance cost compared to cars (Chiun et al. 2009). Malaysia and Thailand have highest user of motorcycles compared to other developing countries. Shown in Figure 1.2, total number of motorcycles are approximately equal to the total number of cars

in Malaysia. Total number of motorcycles are accounts for 49.76% of total numbers of vehicles in Malaysia, raised the awareness to improve the inefficient four stroke motorcycle engines that are carbureted, small scaled and low tech (Jih Houh 2012).

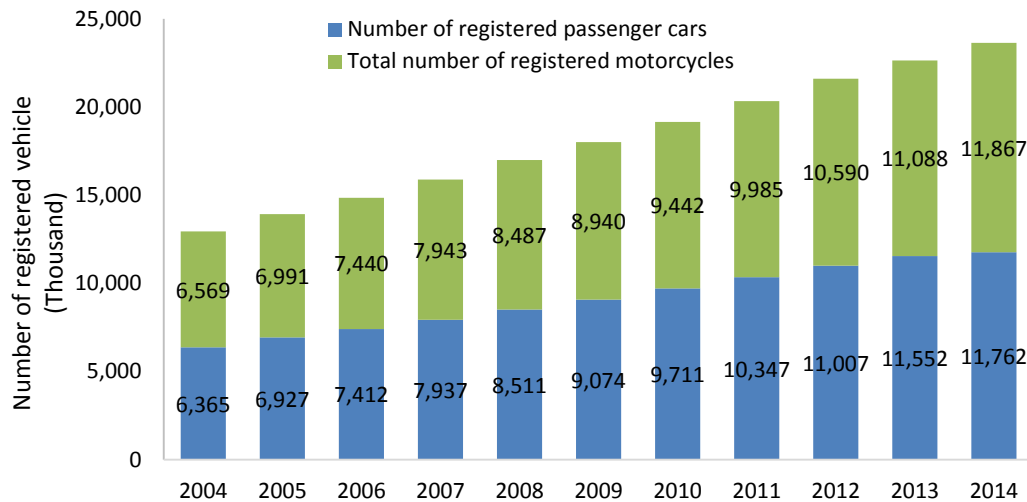


Figure 1.2: Motorcycles and car ownership in Malaysia (Asean Japan Transportation Partnership 2014)

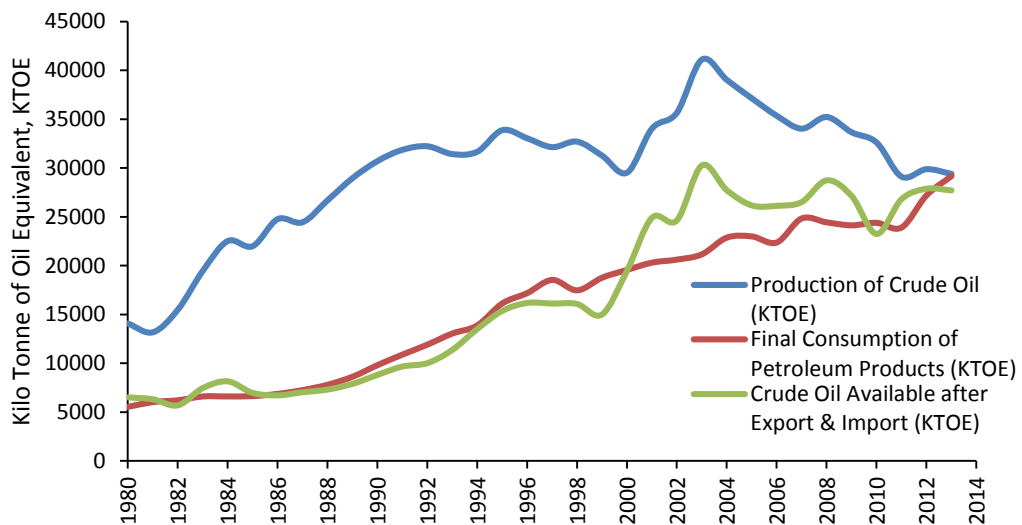


Figure 1.3: Final consumption of Petroleum Products and Crude Oil production in Malaysia (MEIH 2011)

As shown in Figure 1.3, increase in vehicle ownership increases final consumption of petroleum products in Malaysia and the trend increases every year but crude oil production in Malaysia reduces after year 2003. Moreover, petrol price increases due to total world crude oil consumption exceeds the production and found